Journal of ELECTRONIC MATERIALS, Vol. 45, No. 1, 2016
DOI: 10.1007/s11664-015-4067-z

Preparation and Electrochemical Performance of $LiNi_{1/3}Co_{1/3}Mn_{1/3}O_2$ Cathode Materials for Lithium-ion Batteries from Spent Mixed Alkaline Batteries

LI YANG[1,2] and GUOXI XI[1,3]

1.—School of Environment, Henan Normal University, Key Laboratory for Yellow River and Huai River Water Environment and Pollution Control, Ministry of Education, Henan Key Laboratory for Environmental Pollution Control, Xinxiang 453007, Henan, People's Republic of China. 2.—Department of Experimental Center, Henan Institute of Science and Technology, Xinxiang 453003, Henan, People's Republic of China. 3.—e-mail: syzxhome@163.com

$LiNi_{1/3}Co_{1/3}Mn_{1/3}O_2$ cathode materials of lithium-ion batteries were successfully re-synthesized using mixed spent alkaline zinc-manganese batteries and spent lithium-ion batteries as the raw materials. These materials were synthesized by using a combination of dissolution, co-precipitation, calcination, battery preparation, and battery charge–discharge processes. The phase composition, morphology, and electrochemical performance of the products were determined by inductively coupled plasma optical emission spectroscopy, infrared spectra, x-ray diffraction, scanning electron microscopy–energy dispersive spectroscopy, and charge–discharge measurements. The results showed that $LiNi_{1/3}Co_{1/3}Mn_{1/3}O_2$ cathode materials could be successfully re-synthesized at optimal preparation conditions of: co-precipitation, pH value of 8, calcination temperature of 850°C, and calcination time of 10 h. Furthermore, the electrochemical results showed that the re-synthesized sample could deliver an initial discharge capacity of up to 160.2 mAh g^{-1} and Coulomb efficiency of 99.8%.

Key words: $LiNi_{1/3}Co_{1/3}Mn_{1/3}O_2$, cathode materials, spent Zn-Mn batteries, spent LIBs, electrochemical performance

INTRODUCTION

Alkaline Zn-Mn batteries and Li-ion batteries (LIBs) are lightweight and have high energy densities, and are therefore used predominantly as electrochemical power sources in many electric devices; these devices include mobile telephones, personal computers, video cameras, and other modern-life appliances.[1,2] China, the most important battery manufacturing region in the world, currently produces over 20 billion Zn-Mn batteries annually.[3] In 2020, the quantity and weight of the spent LiBs may surpass 25 billion units and 500,000 metric tons,[4] respectively. Correspondingly, the same number of spent batteries, each containing a corrosive electrolytic solution, will be discarded as waste after their lifespan. These spent batteries contain metals such as Ni, Co, Cu, and Li, and produce large amounts of metal-containing hazardous waste. For example, the purity of the MnO_2 and $LiCo_2O_4$ is 88.9% and 83.13% in the cathode materials of spent Zn-Mn batteries and LIBs, respectively.[5,6] Furthermore, the toxic, and possibly explosive, electrolytes used in these batteries are harmful to both the environment and the public.[7–9] Recycling the spent batteries is therefore essential. In order to recycling the spent batteries, the authors have focused on the search of new cathode materials ($LiNi_{1/3}Co_{1/3}Mn_{1/3}O_2$) with higher energy and power density, higher safety and lower cost.

Many types of batteries are used in various fields, and accordingly diverse methods have been used to treat spent batteries.[10–16] However, most reports

(Received July 16, 2015; accepted September 18, 2015; published online October 20, 2015)

have focused exclusively on the recycling of single spent batteries, and the recovery of alkaline batteries has been neglected. This stems mainly from the fact that different types of batteries consist of differing cathode and anode components. Therefore, in order to recycle mixed waste batteries, suitable recycling technologies must be developed for the handling of spent mixed batteries. From the environmental and economic viewpoint, a comprehensive understanding of the current status of recycling of different types of spent batteries is essential to recycling mixed spent batteries in the future.

The challenge lies in performing hybrid recycling that is tailored to the different parts of the various types of batteries, which comprise the mixed spent batteries and obtaining high-value-added products;[17] this tailoring will help to reduce mutual interference among the batteries. As such, selective sorting of the spent batteries by a safe, rapid, and inexpensive method is crucial to preventing important components from being discarded.

The $Ni_xCo_yMn_z$ material is an excellent cathode material, which has been used increasingly in the LIB industry.[18–21] For example, Eglitis reported that $Li_2Co_1Mn_3O_8$ allowed the achieving of very high, voltages.[22] These materials are typically prepared from a pure and relatively expensive chemical reagent. Furthermore, a shortage of raw materials and increased costs of chemical reagents, highlight the need for preparing $Ni_xCo_yMn_z$ cathode materials by recycling valuable metals from spent batteries.

This paper describes the first-ever successful method of synthesizing high-value-added $LiNi_{1/3}Co_{1/3}Mn_{1/3}O_2$ cathode materials by simultaneously recycling spent Zn-Mn batteries and spent LIBs;[23] the method described here differs from the conventional method of obtaining a single metal or its oxide.[24–27] The synthesized $LiNi_{1/3}Co_{1/3}Mn_{1/3}O_2$ cathode materials exhibit cycling performance and high Coulomb efficiency. More importantly, the entire preparation process is environmentally friendly and has the potential to reduce the production costs of cathode materials of LIBs.[28]

MATERIALS AND METHODS

Materials and Reagents

The spent Zn-Mn batteries and spent LIBs ($LiCo_2O_4$) used in this study were kindly supplied from the waste collection stations of Henan Normal University campus in Xinxiang, China. The compound *N*-methyl-2-pyrrolidone (NMP) was used as an ultrasonic solvent to separate the $LiCo_2O_4$ active material from the Al foil. Analytical grade nitric acid, hydrogen peroxide, sodium hydroxide, manganese nitrate, cobalt nitrate, nickel nitrate, and lithium carbonate were all used without further purification. An ultrapure water system (SG Ultra Clear System, Wasseraufbereitung und Regenerierstation, Germany) was used to produce ultrapure water with a specific conductivity of 0.055 μS/cm, for use as the ultrasonic solvent.

Recovery of the Cathode Active Materials and Preparation of the $LiNi_{1/3}Co_{1/3}Mn_{1/3}O_2$ Cathode Materials

The flow chart in Fig. 1 outlines the synthesis of $LiNi_{1/3}Co_{1/3}Mn_{1/3}O_2$ cathode materials from the mixed spent Zn-Mn batteries and spent LIBs. The spent batteries were discharged by connecting the positive and negative poles (to prevent short-circuiting and self-ignition) and then manually dismantled into the anode, cathode, plastic casing, and separators. The cathode materials of the spent LIBs consisted of the $LiCo_2O_4$ active material, carbon-conducting additives (acetylene black), and the binder polyvinylidene fluoride (PVDF) pasted on Al foil. These materials were cut into small pieces using scissors, and sonicated in NMP for 3 min in order to separate the active materials from the foil. Similarly, the MnO_2 electrode materials were obtained by manually disassembling spent Zn-Mn batteries. Next, 3.5 g of the $LiCo_2O_4$ cathode materials and 3.5 g of MnO_2 electrode materials were then dissolved in a 6 mol L^{-1} nitric acid solution (100 mL) containing 2.5 wt.% hydrogen peroxide.[29,30] After the reaction, the solution was filtered and Li, Co, Ni, and Mn concentrations of 10.8, 26.8, 6.05, and 30.4 mg mL^{-1}, respectively, were determined by inductively coupled plasma optical emission spectrometry (ICP-OES). Suitable amounts of

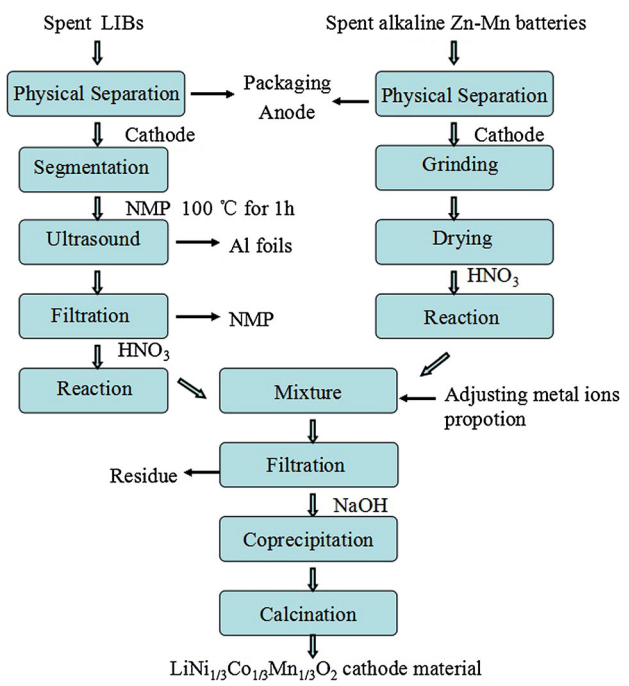

Fig. 1. The synthesis of $LiNi_{1/3}Co_{1/3}Mn_{1/3}O_2$ cathode materials from mixed spent Zn-Mn batteries and spent LIBs.

analytical purity nickel nitrate, cobalt nitrate, and manganese nitrate were added in order to adjust the concentrations of Ni, Co, and Mn (cationic ratio of Ni/Co/Mn = 1:1:1) to prepare $LiNi_{1/3}Co_{1/3}Mn_{1/3}O_2$ cathode materials. Drops totaling 2.5 mol L^{-1} of sodium hydroxide solution, for use as a precipitating agent, were stirred into a mixed aqueous solution in order to adjust the pH values (pH 8); the mixed solution was continuously and vigorously stirred and held at 65°C until a suspension formed. The $Ni_{1/3}Co_{1/3}Mn_{1/3}(OH)_2$ was obtained from the repeated washing and filtering of the suspension, followed by drying at 135°C for 5 h. The $Ni_{1/3}Co_{1/3}Mn_{1/3}(OH)_2$ was then well-mixed with Li_2CO_3 (1.1 times the stoichiometric ratio of $Ni_{1/3}Co_{1/3}Mn_{1/3}(OH)_2$), sintered in air for 10 h at 850°C, and uniformly ground, thereby yielding the $LiNi_{1/3}Co_{1/3}Mn_{1/3}O_2$ cathode materials.

Material Characterization

The amount of Li, Co, Ni, and Mn in the leaching solution was determined by ICP-OES (Optima 2100DV, USA). Using the KBr pellet method, the infrared (IR; TENSOR-27, Germany) spectra of the samples were measured at wavenumbers of 400–4000 cm^{-1} by a spectrophotometer. The samples were characterized by x-ray diffraction (XRD; BRUKER.axs, Germany) with a Cu K_α radiation source. Furthermore, the morphology and the elemental distribution of the samples were determined by using a scanning electron microscope (SEM; Quanta-200, FEI, The Netherlands) equipped with energy dispersive x-ray spectrometry (EDS; INCA 250x; Oxford Instruments, Oxford, UK) capabilities. The electrode was fabricated by coating the slurry of a mixture containing the synthesized sample (type CR2025), acetylene black, and PVDF, in a weight ratio of 8:1:1, onto circular Al current collector foils. Metallic Li foil was used as the counter electrode and the cells were assembled in an Ar-filled glove box. In addition, 1 M $LiPF_6$ dissolved in ethyl carbonate and dimethyl carbonate (1:1 in volume) was used as the electrolyte and the separator. Constant-current charge and discharge experiments were performed in a voltage range of 2.8–4.6 V, using Land battery testers (Land CT2001A; Wuhan, China).

RESULTS AND DISCUSSION

The Effect of pH Value on the IR Spectra of $LiNi_{1/3}Co_{1/3}Mn_{1/3}O_2$ Cathode Materials

The entire exchange process and the final product were affected when various gels or precipitating agents were used in the sol–gel or precipitation reaction process; this effect resulted from the differing polarity of the gels or precipitating agents and the manner in which active ions were obtained. For example, when only water was used as the solvent, no other organic active substances were involved in the formation of the precursor. In that case, a gel is formed or precipitation occurs owing to the crosslinking reaction among the samples; this reaction occurs via the adjacent hydrogen bonds that become connected during the continuous heating, stirring, and evaporation of the solvent. Furthermore, when used as a solvent and a gel agent, respectively, the strong polymerization between anhydrous ethanol or ethylene glycol and citric acid results in the formation of a continuous three-dimensional network. In this work, the crosslinking reaction of the samples occurred mainly through the connected adjacent hydrogen bonds since only NaOH solution was added. The IR spectra of $LiNi_{1/3}Co_{1/3}Mn_{1/3}O_2$ calcined at 850°C and various pH values are shown in Fig. 2A. The absorption peak at 3481 cm^{-1} in Fig. 2A(a, b), corresponds to the OH stretching vibration, which stems mainly from the amount of intramolecular

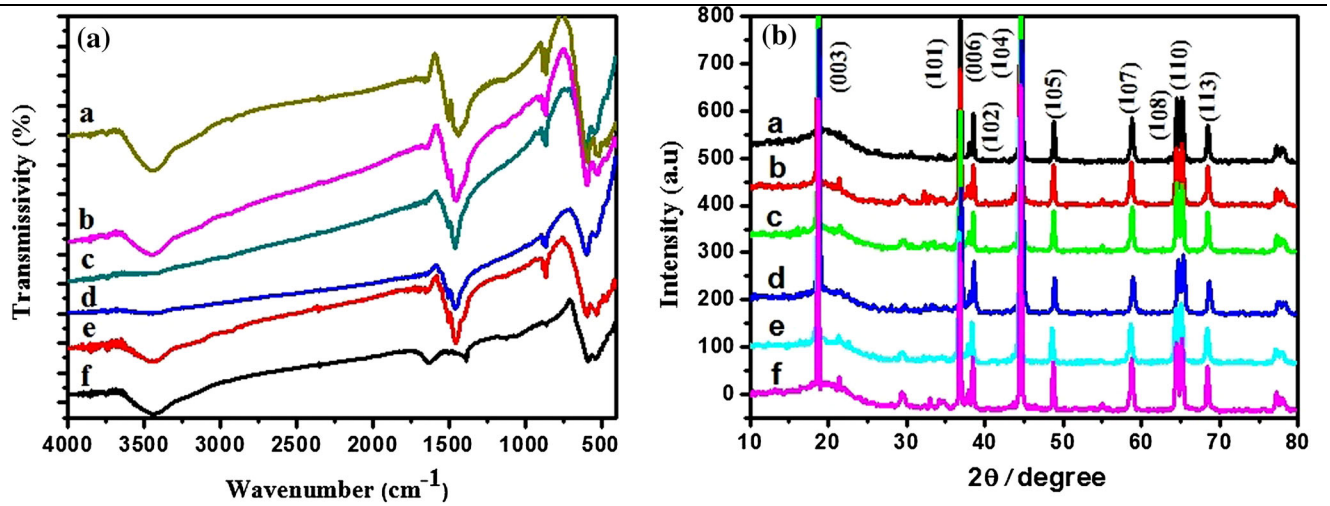

Fig. 2. (A) IR spectra and (B) XRD results of $LiNi_{1/3}Co_{1/3}Mn_{1/3}O_2$ cathode materials prepared at a calcination temperature of 850°C and pH values of *a* pH 5, *b* pH 6, *c* pH 7, *d* pH 8, *e* pH 9, and *f* pH 10.

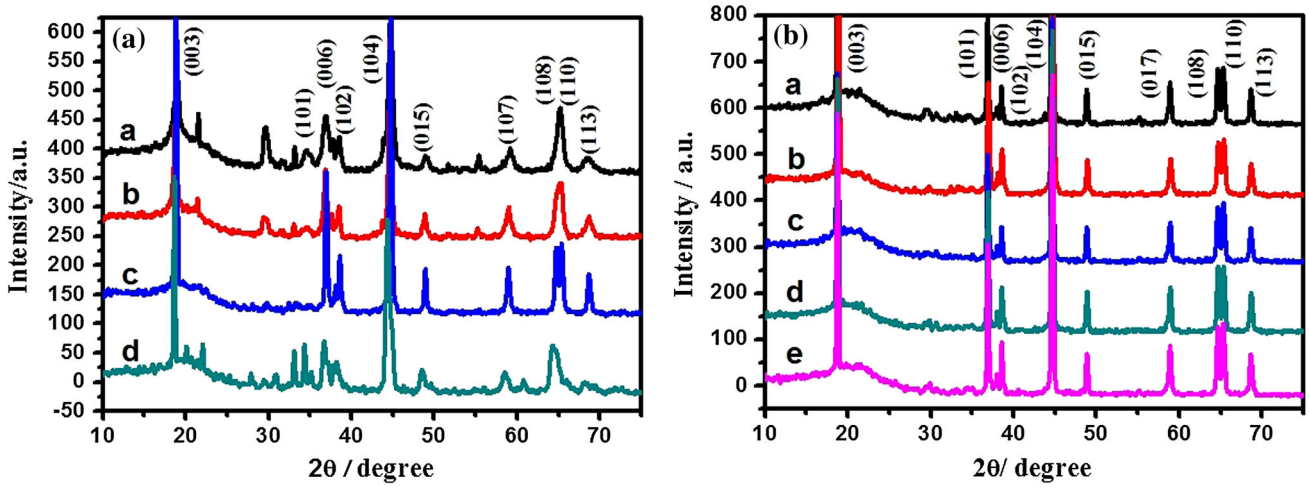

Fig. 3. (A) XRD patterns of $LiNi_{1/3}Co_{1/3}Mn_{1/3}O_2$ cathode materials prepared at various calcination temperatures (*a* 650°C, *b* 750°C, *c* 850°C, *d* 950°C). (B) XRD patterns of $LiNi_{1/3}Co_{1/3}Mn_{1/3}O_2$ cathode materials prepared at various calcination times (*a* 7 h, *b* 8 h, *c* 9 h, *d* 10 h, *e* 11 h).

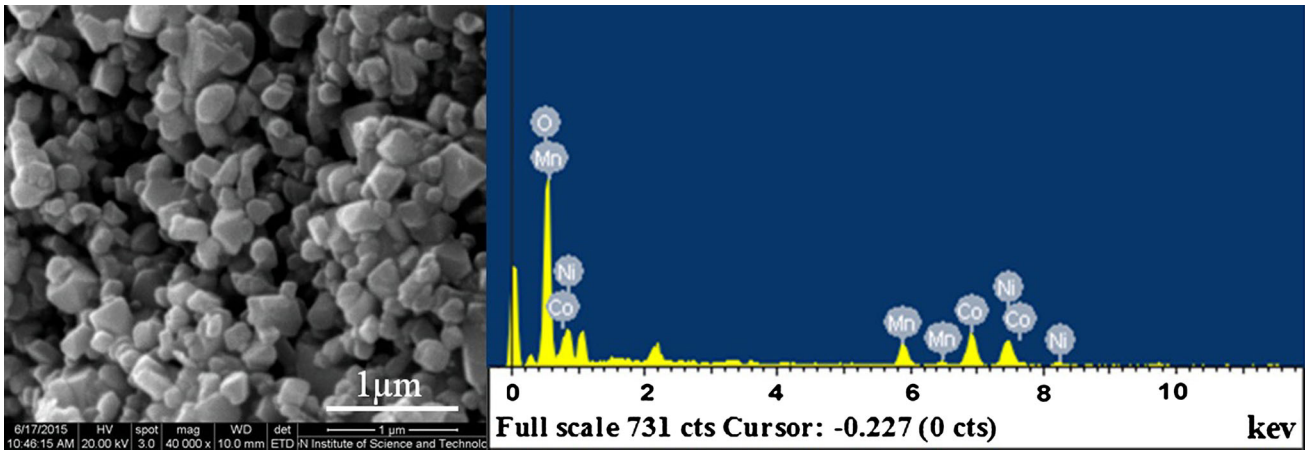

Fig. 4. SEM micrograph and EDS spectrum of the $LiNi_{1/3}Co_{1/3}Mn_{1/3}O_2$ cathode materials prepared.

crystalline water contained in the co-precipitation products; this water resulted from the excess water solvent. The OH was involved in the co-precipitation reaction that resulted in the spectrum shown in Fig. 2A(c, d). Moreover, the re-emergence of the absorption peak corresponding to the OH stretching vibration (Fig. 2A(e, f)) with increased pH values, confirms that excess OH was formed during the reaction. In contrast, the absence of peaks corresponding to impurities and the sharp peak at 625 cm^{-1} in Fig. 2A(d), indicate that pure $LiNi_{1/3}Co_{1/3}Mn_{1/3}O_2$ cathode materials are formed at a pH value of 8.

The Effect of pH Value on the XRD Spectra of $LiNi_{1/3}Co_{1/3}Mn_{1/3}O_2$ Cathode Materials

As Fig. 2B shows, the XRD peaks of $LiNi_{1/3}Co_{1/3}Mn_{1/3}O_2$ cathode materials are basically the same irrespective of pH value, and the main phase exhibits peaks which are characteristic of ternary materials. In contrast, the peaks corresponding to impurities vary significantly with pH value (5, 6, 7, 9, 10), for 2θ values of 30°–35°. The characteristic peak of the $LiNi_{1/3}Co_{1/3}Mn_{1/3}O_2$ cathode materials occurs prominently at a pH value of 8, however, and the peaks corresponding to impurities are no longer observed.

The Effect of Calcination Temperature on the $LiNi_{1/3}Co_{1/3}Mn_{1/3}O_2$ Cathode Materials Prepared

As Fig. 3A shows, the characteristic XRD peaks of the $LiNi_{1/3}Co_{1/3}Mn_{1/3}O_2$ cathode materials are not completely formed (Fig. 3A(a, b)) at calcination temperatures below 750°C, but many secondary phases are formed. In addition, identifying the phases present at temperatures higher than 950°C was difficult owing to the agglomeration resulting from the shrinkage of micro pores during the crystallization process (Fig. 3A(d)). Therefore, 850°C was selected as the optimum calcination tempera-

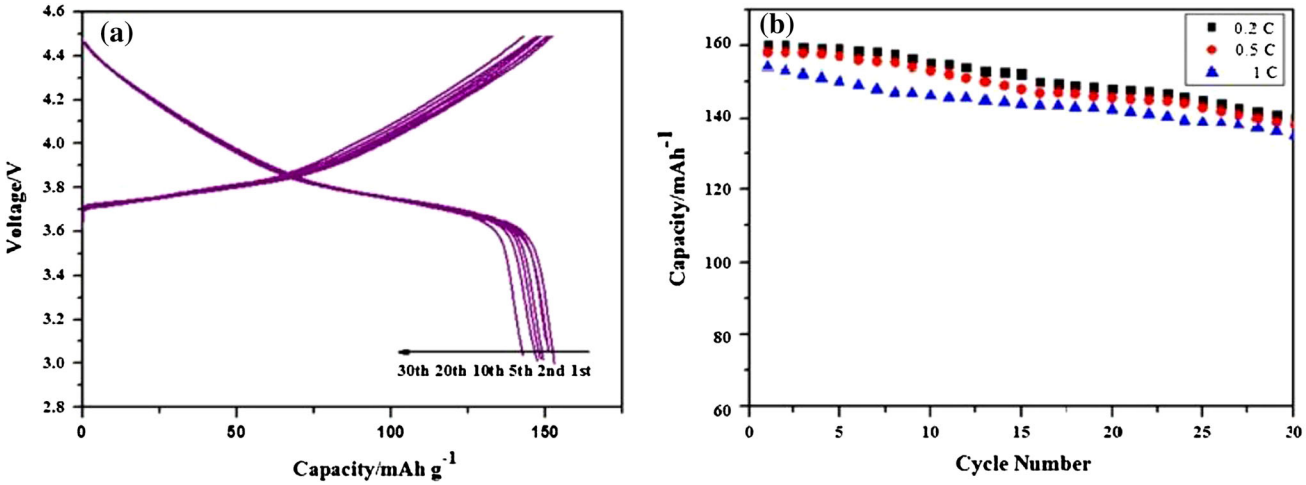

Fig. 5. (A) Charge/discharge profiles of the first 30 cycles of the re-synthesized sample at 0.1 C and a voltage range of 2.8–4.6 V. (B) Cycling performance of $LiNi_{1/3}Co_{1/3}Mn_{1/3}O_2$ cells charged at 0.2 C, 0.5 C, and 1 C.

ture of the $LiNi_{1/3}Co_{1/3}Mn_{1/3}O_2$ cathode materials shown in Fig. 3A(c).

The Effect of Calcination Time on the $LiNi_{1/3}Co_{1/3}Mn_{1/3}O_2$ Cathode Materials Prepared

Figure 3B shows the XRD patterns of the materials calcined for various times (7 h–11 h) at 850°C. As the figure shows, increased amounts of the materials are formed with increasing calcination time. Moreover, owing to an increase in the crystallite size, the peaks become sharpened with prolonged calcination at high temperatures. The patterns changed only slightly, however, for calcination times greater than 10 h. Therefore, 10 h was considered the optimum calcination time of $LiNi_{1/3}Co_{1/3}Mn_{1/3}O_2$ cathode materials calcined at 850°C.

An SEM micrograph and EDS spectrum of the $LiNi_{1/3}Co_{1/3}Mn_{1/3}O_2$ cathode materials are shown in Fig. 4. The micrograph reveals a smooth surface with a well-dispersed structure of ~0.1-μm-sized particles, although a few agglomerations exist. This may be attributed primarily to the influence of pH value on the precursor during the co-precipitation reaction as well as the effect of calcination temperature and calcination time. The composition, proportion, and element distributions of the $LiNi_{1/3}Co_{1/3}Mn_{1/3}O_2$ cathode materials were determined by EDS. The spectrum shows that the materials consist of the expected elements and the amount of each element is consistent with the stoichiometric ratio, as dictated by the ratio of the elements in the molecular formula.

Electrochemical Performance

In order to systematically evaluate the electrochemical performance of the $LiNi_{1/3}Co_{1/3}Mn_{1/3}O_2$ cathode materials, charge/discharge profiles of the 1st, 2nd, 3rd, 10th, 20th, and 30th cycles of the $LiNi_{1/3}Co_{1/3}Mn_{1/3}O_2$ cells were measured; the rate capability and cyclability of the cells were also determined, as shown in Fig. 5A. At 0.1 C, the synthesized materials have an initial discharge-specific capacity and Coulomb efficiency of 160.2 mAh g^{-1} and 99.9%, respectively, as shown in Fig. 5A; i.e., the materials exhibit an excellent cycling performance and have a high Coulomb efficiency. In addition, an excellent rate capability is an important and highly desirable feature in secondary battery applications. Figure 5B shows the rate capability and cyclability of the $LiNi_{1/3}Co_{1/3}Mn_{1/3}O_2$ cathode materials at voltages of 2.8–4.6 V and various C-rates. These materials delivered a high specific capacity of 158.3, 155.6, and 148 mAh g^{-1}, and corresponding 30th-cycle discharge capacities of 140.2, 138.4, and 135.3 mAh g^{-1} at 0.2, 0.5, and 2.0 C, respectively. Therefore, the synthesized $LiNi_{1/3}Co_{1/3}Mn_{1/3}O_2$ cathode materials have high discharge specific capacity and good rate capability, and exhibit excellent cycling performance.[31]

CONCLUSION

$LiNi_{1/3}Co_{1/3}Mn_{1/3}O_2$ cathode materials were successfully re-synthesized through a combination of dissolution, co-precipitation, calcination, battery preparation, and battery charge–discharge processes; the acid leaching solution from the mixed spent alkaline Zn-Mn batteries and spent LIBs were used as raw materials. This study utilized different types of batteries containing various metal elements and proposed a novel method of synthesizing high-value-added $LiNi_{1/3}Co_{1/3}Mn_{1/3}O_2$ cathode materials rather than its oxide or single metal. The synthesized materials exhibit excellent cycling performance and have high Coulomb efficiency.

HIGHLIGHTS

- $LiNi_{1/3}Co_{1/3}Mn_{1/3}O_2$ cathode materials of lithium-ion batteries were successfully re-synthesized using mixed spent alkaline zinc-manganese batteries and spent lithium-ion batteries.
- The products were characterized by ICP-OES, IR, XRD, SEM–EDS techniques and electrochemical performance.
- The electrochemical results showed that the re-synthesized sample could deliver an initial discharge capacity of up to 160.2 mAh g^{-1}.
- A novel way was used to recycle mixed spent alkaline.
- The target product is not a single metal or its oxide but high-value-added cathode materials.

ACKNOWLEDGEMENTS

The authors are thankful to financial support obtained from the National Natural Science Foundation of China (Grant No. 51174083), (Grant No. 51304064) and the Doctoral Fund of the Ministry of Education of China (20114104110004).

REFERENCES

1. L. Li, G.S. Zeng, S.L. Luo, X.R. Deng, and Q.J. Xie, *J. Korean Soc. Appl. Biol. Chem.* 56, 187 (2013).
2. Y. Ma, Y. Cui, X.X. Zuo, S.N. Huang, K.S. Hu, X. Xiao, and J.M. Nan, *Waste Manag.* 34, 1793 (2014).
3. D. Espinosa, A. Bernardes, and J. Tenório, *J. Power Sources* 135, 311 (2004).
4. X.L. Zeng, J.H. Li, and Y.S. Ren, *IEEE. I. Symp. Sustain. Syst. Technol.* 1 (2012).
5. G.X. Xi, M.X. Lu, and L. Yang, *Environ. Prot. Chem. Ind.* 25, 379 (2005).
6. L. Yang, G.X. Xi, and Y.B. X, *Ceram. Int.* 41, 11498 (2015).
7. D. Lisbona and T. Snee, *Process Saf. Environ. Prot.* 89, 434 (2011).
8. D.H.P. Kang, M. Chen, and O.A. Ogunseitan, *Environ. Sci. Technol.* 47, 5495 (2013).
9. H. Aral and A. Vecchio-Sadus, *Ecotoxicol. Environ. Saf.* 70, 349 (2008).
10. A. Babakhani, F. Rashchi, A. Zakeri, and E. Vahidi, *J. Power Sources* 247, 127 (2014).
11. G. Belardi, F. Medici, and L. Pig, *J. Power Sources* 248, 1290 (2014).
12. S.Y. Choi, V.T. Nguyen, J.C. Lee, H. Kang, and B.D. Pandey, *J. Hazard. Mater.* 278, 258 (2014).
13. Y. Ma, Y. Cui, X.X. Zuo, S.N. Huang, K.S. Hu, X. Xiao, and J.M. Nan, *Waste Manag.* 34, 1793 (2014).
14. W. Waag, C. Fleischer, and D.U. Sauer, *J. Power Sources* 258, 321 (2014).
15. X.L. Zeng and J.H. Li, *J. Hazard. Mater.* 271, 50 (2014).
16. M.V. Gallegos, L.R. Falco, M.A. Peluso, J.E. Sambeth, and H.J. Thomas, *Waste Manag.* 33, 1483 (2013).
17. M. Buzatu, S.S. Aceanu, M.I. Petrescu, G.V. Ghica, and T. Buzatu, *J. Power Sources* 247, 612 (2014).
18. C.H. Zhao, X.X. Wang, R. Liu, X.R. Liu, and Q. Shen, *Ionics* 20, 645 (2014).
19. H. Liu, C. Chen, C.Y. Du, X.S. He, G.P. Yin, B. Song, P.J. Zuo, X.Q. Cheng, Y.L. Ma, and Y.Z. Gao, *J. Mater. Chem. A* 3, 2634 (2015).
20. Z.Y. Wang, E.Z. Liu, C.N. He, C.S. Shi, J.J. Li, and N.Q. Zhao, *J. Power Sources* 236, 25 (2013).
21. J. Gao, Z.L. Huang, J.J. Li, X.M. He, and C.Y. Jiang, *Ionics* 20, 301 (2014).
22. R.I. Eglitis and G. Borstel, *Phys. Stat. Solidi (a)* 202, R13 (2005).
23. L. Li, X.X. Zhang, R.J. Chen, T.L. Zhao, J. Lu, F. Wu, and K. Amine, *J. Power Sources* 249, 28 (2014).
24. R. Rácz and P. Ilea, *Hydrometallurgy* 139, 116 (2013).
25. C.Y. Hu, J. Guo, J. Wen, and Y.X. Peng, *J. Mater. Sci. Technol.* 29, 215 (2013).
26. J. Formanek, J. Jandova, and J. Capek, *Hydrometallurgy* 138, 100 (2013).
27. M. Buzatu, S.S. Aceanu, M.I. Petrescu, G.V. Ghica, and T. Buzatu, *J. Power Sources* 247, 612 (2014).
28. E. Gratz, Q. Sa, D. Apelian, and Y. Wang, *J. Power Sources* 262, 255 (2014).
29. G.X. Xi, L. Yang, and M.X. Lu, *Mater. Lett.* 60, 3582 (2006).
30. L. Yang, Q.H. Yan, G.X. Xi, L.Y. Niu, T.J. Lou, T.X. Wang, and X.S. Wang, *J. Mater. Sci.* 46, 6106 (2011).
31. Z.Y. Wang, Y. Zhang, B.J. Chen, and C. Lu, *J. Solid State Electrochem.* 18, 1757 (2014).